

## MAGNETIC-FIELD EFFECT ON HEAT TRANSFER WITHIN A CATHODE ARC SPOT

A. M. Esipchuk,<sup>a</sup> A. Marotta,<sup>a</sup> and  
L. I. Sharakhovskii<sup>b</sup>

UDC 621.387.143.014.31

*The authors present results of an experimental study of the heat flux within the arc spot of the copper cathode of an electric-arc heater with magnetic-field-induced displacement of the arc in an air medium – one of the most important parameters determining the erosion and service life of such a cathode. The investigations were carried out at a current strength of 110–450 A, a magnetic induction of 0.009–0.38 T, and atmospheric pressure.*

**Introduction.** Electric-arc discharges find wide application for heating of gases in electric-arc heaters used in various spheres of science and technology. An electric current is transferred from an electric-arc plasma to the electrodes of electric-arc heaters via special confined regions of the electrode surface, which are called arc spots. In the latter, intense heat fluxes always occur, which inevitably cause destruction of the electrodes. The highest densities of the heat flux and the highest level of erosion are characteristic of so-called "cold" electrodes manufactured from metals with a relatively low melting temperature, for instance, copper. Therefore, for the development of methods of electrode protection against rapid destruction, it is rather urgent to investigate the thermal regime of such electrodes. A copper cathode has the highest current density and the shortest service life in electric-arc heaters. The thermal balance for an arc cathode can be represented in general form [1] by the following relation:

$$(1 - \alpha)(\epsilon \Delta U_c + U_i - \phi_0) - \alpha \phi_- - \rho' - \zeta - \xi + \xi' + \eta + \varphi = 0. \quad (1)$$

To make the goal and the procedure of this investigation more lucid, we will characterize the main terms entering Eq. (1):  $\alpha$  is the fraction of the current carried by electrons;  $\epsilon$  is the fraction of the ionic energy transferred to the cathode;  $\Delta U_c$  is the near-cathode voltage drop;  $U_i$  is the ionization potential;  $\phi_0$  is the normal work function of the cathode material;  $\phi_-$  is the effective work function (which is lower than  $\phi_0$  due to the presence of a high-intensity electric field in the near-electrode region);  $\rho'$  is the cathode cooling due to radiation;  $\zeta$  is the heat loss by evaporation from the cathode material;  $\xi$  is the heat transferred to the cathode by conduction;  $\xi'$  is the heat loss from the cathode to the gas by conduction and convection;  $\eta$  is the energy supplied to the cathode by the external source;  $\varphi$  is the energy transfer by uncharged carriers that is induced by electrons accelerated in the near-cathode region. Many terms of Eq. (1) are seen to have large indeterminacies in their values. Only some of them, such as the ionization potential, the work function of the cathode material, and the near-electrode potential drop, can be considered to be known to a sufficient degree. However, the near-electrode potential drop is measured only for a limited category of arc discharges, namely, in steady-state arcs. Its determination in arcs moving with a large velocity as, for instance, in electric-arc heaters is a very complicated task and up to now it has not been measured. To provide rapid displacement of the arc in an electric-arc heater, a magnetic field or an eddy gas flow is used as a rule, but the highest arc velocities are achieved with the aid of a magnetic field.

---

<sup>a</sup>Gleb Wataghin Institute of Physics at Campinas State University, Campinas, Brazil (Instituto de Física "Gleb Wataghin," Universidade Estadual de Campinas, Unicamp, 13083-970, Campinas, São Paulo, Brasil); <sup>b</sup>Academic Scientific Complex "A. V. Luikov Heat and Mass Transfer Institute," National Academy of Sciences of Belarus, Minsk, Belarus. Translated from *Inzhenerno-Fizicheskii Zhurnal*, Vol. 73, No. 6, pp. 1245-1254, November–December, 2000. Original article submitted March 22, 2000.

Therefore, at present the most adequate data on the heat fluxes within arc spots can be obtained by thermophysical methods that instrumentally take into account the integral effect of all the components of the energy balance presented in relation (1). Some of these methods are described in [2]. Below we undertake additional checking of the measurement results presented in [2], where the authors have revealed a dependence of the heat fluxes toward a cathode spot on the magnetic field, which is very important for electric-arc heaters with an arc displaced by a magnetic field.

In a macroscopic model of erosion of cold electrons [3], the notion of the thermal volt-equivalent of an arc spot  $U$  is widely used, by which the ratio of the heat flux within an arc spot to the strength of the current is meant:  $U = Q/I$ . The volt-equivalent is one of the important parameters specifying the thermal regime of an arc spot and thus the erosion of an electrode, which is well seen from the expression for the specific erosion  $g$  (in kg/C) presented in the indicated model [3, 4]:

$$g = g_0 + \frac{UW(f(U))}{h_{\text{ef}}}. \quad (2)$$

Here,  $g_0$  is the specific "microerosion" in a spot of the first kind according to the known classification developed by V. I. Rakhovskii (see [5, 6]). The macroscopic model considers erosion as a process of ablation of the electrode material under the action of the intense heat fluxes within an arc spot [3, 4]. In Eq. (2),  $W(f(U))$  is the dimensionless enthalpy of ablation, being a function of the dimensionless criterion  $f(U)$ . The latter characterizes the degree of fusion of the electrode surface in a spot and the type of cathode spot (a spot of the first or second kind, see [5, 6]). In addition to the energy characteristics of the spot, such as the thermal volt-equivalent  $U$ , the strength of the current  $I$ , and the current density  $j$ , the criterion  $f(U)$  includes the thermophysical parameters of the cathode material  $T_f$ ,  $\lambda$ , and  $a_1$ , the arc velocity  $v$ , and the electrode temperature  $T$  [3]:

$$f(U) = \frac{\pi^{1.5} v \lambda^2 (T_f - T)^2}{8 a_1^{1.5} U^2 I^{0.5}}. \quad (3)$$

According to [3], for  $f(U) > 1$ , the function  $W(f(U)) = 0$ ; here  $g = g_0$  and "microerosion" characterized approximately by a constant value ( $g_0 \approx 2-3 \mu\text{g/C}$ ) occurs within a spot of the first kind. For  $f(U) < 1$ , variable "macroerosion" is observed within a spot of the second kind, which is a function of the dimensionless heat of erosion  $W(f(U))$ . Here, the form of the function  $W(f(U))$  depends on the mode of arc-spot movement: continuous or intermittent (step-by-step) (see [4]). Thus, according to [3, 4], the volt-equivalent  $U$  should be referred to the paramount parameters determining the transitions of erosion from one mode to another and the specific erosion itself for  $f(U) < 1$ . This characterizes its importance for investigation of the erosion process as a whole. According to [2], the quantity  $U$  is close to the value of the near-cathode voltage drop  $\Delta U_c$ .

The present work is concerned with measurement of the thermal volt-equivalent  $U$  of a copper electrode and its dependence on the magnetic field. This dependence is important since it leads to the existence of an optimum value of the field, exceeding which can entail an increase in the extent of erosion of the electrodes of electric-arc heaters. Data on the thermal volt-equivalent of a copper cathode as a function of the magnetic field must be refined first of all for calculations of the optimum operating conditions of the "cold" cathode in electric-arc heaters with minimum erosion [7].

**Experimental Setup and Measurement Method.** Experiments on measurement of the thermal volt-equivalent of an arc spot on a copper cathode in an air medium have been carried out on the experimental setup of the Gleb Wataghin Institute of Physics at Campinas University (GWIPh) (Brazil) that is depicted in Fig. 1. The setup consists of two uncooled coaxial ring electrodes (1 and 4) placed in an axial magnetic field induced by two solenoids 6. Under the action of the Lorentz force the arc moves around the electrodes in the azimuthal direction with a large velocity (tens and hundreds of meters per second).

An arc was initiated in the gap between the cathode and the anode by breaking the circuit formed by auxiliary cathode 5 and anode 4 using a special solenoid. In so doing, an auxiliary arc developed in the gap

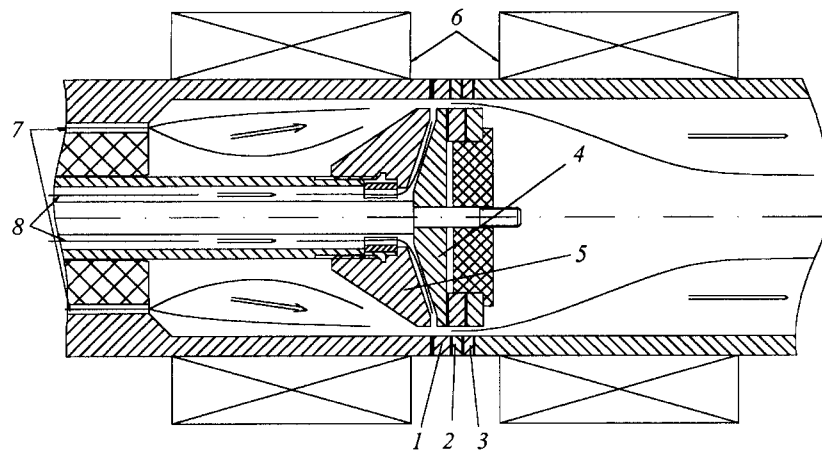


Fig. 1. Schematic of the experimental setup: 1) cathode; 2, 3) electroneutral calorimetric rings; 4) anode; 5) starting electrode; 6) solenoids; 7) basic gas; 8) auxiliary gas.

between them. In the same gap, via the axial channel in the internal electrode a small amount of air (approximately 4% of the main flow rate) was supplied that blew out the auxiliary arc into the gap between the main electrodes 1 and 4. After initiation of the main arc, due to its sharply decreasing volt-ampere characteristic, the voltage between the electrodes decreased to such an extent that the small-current auxiliary arc was spontaneously extinguished since it was connected in the circuit in parallel with the main arc via a ballast resistor. This allowed us to avoid high-voltage ignition, which is a significant hazard to sensitive measurements by the thermocouples used in the experiments for recording the electrode temperature.

To measure the heat flux  $Q_s$  arriving at the electrode via the cathode spot, we placed up against cathode 1 two narrow auxiliary copper electroneutral rings 2 and 3 of width 3 mm each, which were separated by thin spacers manufactured from a heat- and electrical-insulating material. To record the temperature, use was made of Chromel–Alumel thermocouples embedded in the lateral face of the cathode and in the auxiliary rings at a distance of 1.5–2.0 mm from their interior surface. The operating time of the experimental setup was 0.6–1.0 sec, depending on the value of the arc current and the magnetic field.

Control of the experimental setup and data acquisition were carried out by a computer using a special program based on the graphical software "LabView" intended for work with test equipment (of the National Instruments Company, USA). The inquiry frequency of each channel in data acquisition was 10 kHz. The following parameters were written on a hard disk of the computer: the arc current, arc voltage, rotational velocity of the arc in the electrode gap, magnetic induction, and temperature of the cathode and the auxiliary rings.

The heat flux through a moving cathode spot cannot be measured by a direct method. We used a calorimetric method that allowed us to obtain it indirectly by determining the total heat fluxes toward three adjacent rings. In this case, a current was conveyed only to ring-electrode 1, and the cathode spot was always within this ring. Rings 2 and 3 were electroneutral. Heat was transferred to them only by radiation and convection from remote regions of the interelectrode plasma, i.e., from the arc column, chamber walls, plasma jet, and anode. If the heat flux arriving at the cathode directly through the arc spot is designated by  $Q_s$ , then the radiative-convective flux incident on the remaining surface of the cathode (outside the spot) is equal to  $Q_1 - Q_s$ , where  $Q_1$  is the measured total heat flux toward the cathode. This radiative-convective flux depends on the geometry of the system (on the heat-absorbing capacity of the ring surface and on the distance to the radiation source, i.e., the arc column), while  $Q_s$  is determined just by the electrode material and the kind of plasma-forming gas. By changing the configuration of the electrode system, in particular, the distance from the heat absorber to the arc discharge, we can find  $Q_s$  as the constant component of the total heat flux  $Q_1$ , which changes as a function of the distance.

The scheme of the distribution of the integral density of the convective and radiative heat fluxes along the setup axis adopted for the calculations is shown in Fig. 2. It was assumed that due to the small width of

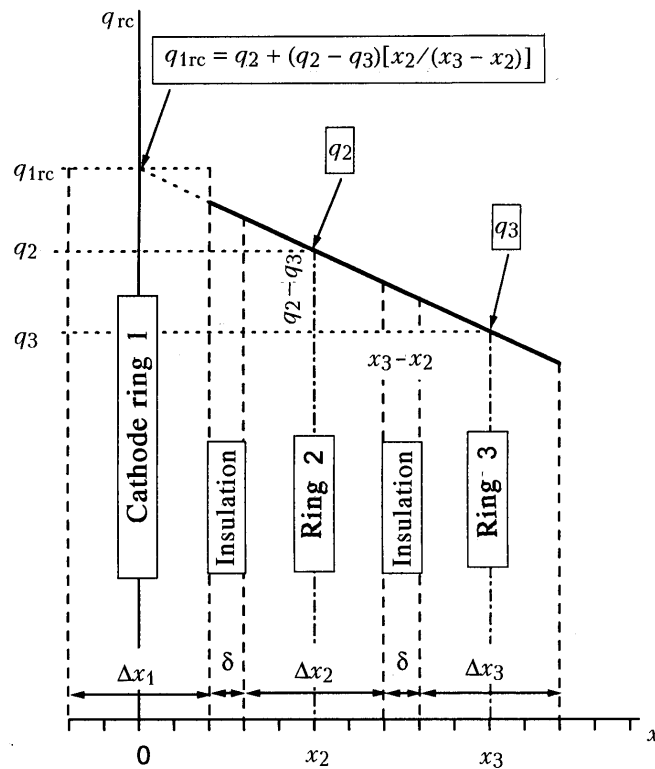


Fig. 2. Diagram of the density distribution of the radiative-convective heat fluxes along the electrode axis adopted for calculating the thermal volt-equivalent of the cathode spot.

the cathode ring the arc spot encountered all points of its surface with equal probability and the density of the total heat flux (from the cathode spot, convection, and radiation) was the same over the entire interior cathode surface. The density of the radiative and convective heat fluxes toward the adjacent electroneutral rings was assumed to decrease linearly with increase in the distance from the arcing zone. The position of the arcing zone in the middle cross section over the width of the cathode ring was taken to be its mean-statistical position, and the coordinate  $x$  was reckoned from the middle cross section of the cathode (see Fig. 2). The assumption of a linear decrease in the convective-radiative heat flux with decrease in the distance from the arcing zone can be made at rather small distances from the cathode, which was fulfilled in the experiment: they were changed from 4 to 8 mm with a diameter of the cathode of 42 mm and of the anode of 36 mm.

As has already been mentioned, to separate  $Q_s$  from the integral heat flux on the cathode, we measured the density of the heat fluxes  $q_i$  toward three adjacent rings 1, 2, and 3 (see Figs. 1 and 2). From the scheme of the heat flux density distribution along the electrodes of the experimental setup (Fig. 2) we can easily write an expression for the density of the radiative-convective heat flux toward the cathode:

$$q_{1rc} = q_2 + (q_2 - q_3) \frac{x_2}{x_3 - x_2}. \quad (4)$$

Since the inside diameter of all the rings in our experiments was the same and the integral heat flux toward the  $i$ -th ring was  $Q_i = q_i F_i$ , then we can obtain an expression for the heat flux supplied to the cathode via the arc spot:

$$\begin{aligned} Q_s &= Q_1 - Q_{1rc} = (q_1 - q_{1rc}) 2\pi R_1 \Delta x_1 = \\ &= \left( q_1 - q_2 - (q_2 - q_3) \frac{x_2}{x_3 - x_2} \right) 2\pi R_1 \Delta x_1. \end{aligned} \quad (5)$$

Taking into account the short duration of the experiment and the negligible heat losses in this time via the exterior and lateral surfaces of the cathode and the auxiliary rings, we can consider them to be heat-insulated on all sides, with the exception of the interior surface, which was in contact with the electric arc and/or the arc plasma. In this case, the temperature field of the ring can be calculated using the known solution of the problem of heating of an infinitely long hollow cylinder with a heat-insulated exterior surface with boundary conditions of the second kind (i.e., with a constant heat flux  $q = \text{const}$ ) on the interior surface. An analytical solution of this problem is presented in [8, 9] in the form

$$\begin{aligned}
T(r, \tau) - T_0 = & \frac{q}{\lambda} R_1 \left\{ \frac{R_1^2}{R_2^2 - R_1^2} \left[ 2 \frac{a\tau}{R_1^2} - \frac{1}{4} \left( 1 - 2 \frac{r^2}{R_1^2} \right) - \right. \right. \\
& \left. \left. - \frac{R_2^2}{R_1^2} \left( \ln \frac{r}{R_2} + \frac{R_1^2}{R_2^2 - R_1^2} \ln \frac{R_1}{R_2} + \frac{3}{4} \right) \right] \right\} + \\
& + \pi \sum_{\sigma} \frac{1}{\sigma} \frac{J_1(\sigma) J_1\left(\sigma \frac{R_2}{R_1}\right)}{J_1^2(\sigma) - J_1^2\left(\sigma \frac{R_2}{R_1}\right)} \left[ J_0\left(\sigma \frac{r}{R_1}\right) Y_1\left(\sigma \frac{R_2}{R_1}\right) - \right. \\
& \left. - Y_0\left(\sigma \frac{r}{R_1}\right) J_1\left(\sigma \frac{R_2}{R_1}\right) \exp\left(-\sigma^2 \frac{a\tau}{R_1^2}\right) \right]. \tag{6}
\end{aligned}$$

Here  $\sigma = \mu R_1$ , where  $\mu$  are the roots of the characteristic equation

$$J_1(\mu R_1) Y_1(\mu R_2) = Y_1(\mu R_1) J_1(\mu R_2). \tag{7}$$

From (6) it is seen that the ring temperature changes nonlinearly with time only at the very beginning of heating, i.e., near  $\tau = 0$ . For a rather large heating time  $\tau$ , the exponential term of the equation becomes negligible and the temperature increases linearly with time. This mode of heat conduction is called regular. Neglecting the exponential term and differentiating (6) with respect to time, we arrive at an expression for the density of the heat flux arriving at the ring in the regular mode:

$$q = \frac{\lambda}{a} \frac{R_2^2 - R_1^2}{2R_1} \frac{dT}{d\tau} = K \frac{dT}{d\tau}, \tag{8}$$

which allows calculation of the density of the heat flux arriving at the ring from its heating rate  $dT/d\tau$  recorded in experiments ( $K$  is the proportionality factor). The heating curves were recorded simultaneously for the indicated three adjacent rings and then the heat-flux densities  $q$  were calculated in each of them.

To measure the volt-equivalent  $U$ , we used cathodes with a thickness of 2 to 3 mm and 3-mm-thick auxiliary rings with an inside diameter of 42 mm and an outside diameter of 52 mm manufactured from commercial copper. This thickness was chosen for the purpose of obtaining more stable results from the viewpoint of repeatability. The use of cathodes of another thickness substantially diminished the repeatability of the results. In the case of a smaller thickness, the result was strongly affected by the durability of the heat insulation; the latter failed too rapidly, exposing the lateral surface of the cathode, which led to overestimated results in measuring the heat flux. For an electrode thickness of 5 mm, the axial displacements of the arc became sensitive and distorted the curve of temperature rise. In all the experiments, the radial gap between the cathode and the anode was held constant and equal to 3 mm. The insulation thickness was varied slightly and depended only on the type of material used. When mica paper was used, it was 0.8 mm, while in the case of asbestos paper PV-J3, it was 1.1 mm. This geometry of the system of cathode–auxiliary rings allowed us to be within

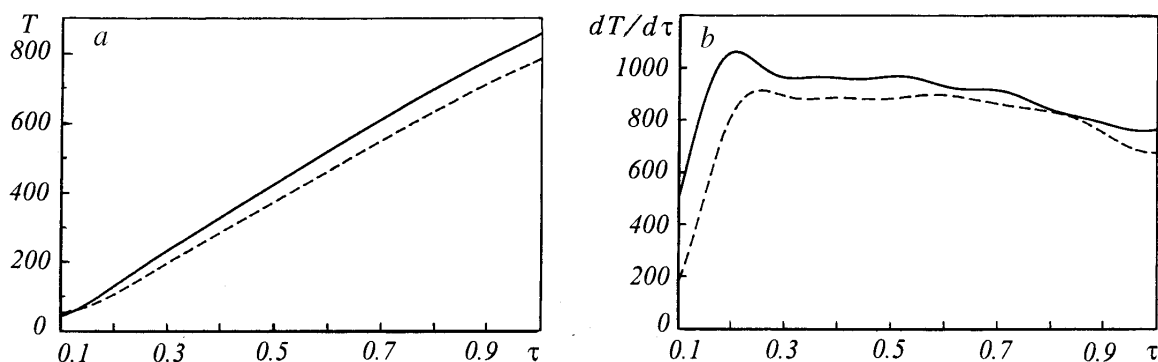


Fig. 3. Traces of the temperature  $T$  of cathode ring 1 (see Fig. 1) (a) and time variation of the derivative  $dT/d\tau$  for them (b). Solid line, signal of the thermocouple placed a distance of 0.9 mm from the interior heated surface; dashed line, at a distance of 3.4 mm.  $T$ , °C;  $\tau$ , sec;  $dT/d\tau$ , deg/sec.

the limits of the assumption of a linear decrease in the heat-flux density. Here, the share of the radiative-convective heat flux with respect to the total heat flux on the cathode was at the level of 30%.

As the plasma-forming gas, use was made of compressed air from an industrial air duct at atmospheric pressure in the discharge chamber without additional cleaning. The main operating parameters were varied within the following ranges: the magnetic field from 0.009 to 0.38 T, the arc current from 110 to 450 A, and the axial velocity of the plasma-forming gas from 0.1 to 1.0 m/sec. Variation of the operating parameters within these ranges allowed us to obtain rather wide limits of change in the velocity of displacement of the arc on the electrode surface, namely, from 28 to 401 m/sec. The experiments were carried out in series, five switchings each without changing the insulation. To decrease the effect of contamination of the electrode surface, the latter was subjected to mechanical decontamination in the interval between arc initiations within one series and to chemical cleaning (washing in a sulfuric acid solution of chromium trioxide followed by drying with compressed air) upon changing the insulation.

**Results and Discussion.** Figure 3a presents characteristic curves of the electrode temperature recorded as a function of time, while Fig. 3b shows its derivative  $dT/d\tau$ , proportional to the density of the heat flux. The dashed line shows the temperature on the lateral electrode surface at a point located at 3.4 mm from its interior surface, and the solid line at a point located at 0.9 mm. Starting from the instant  $\tau = 0.3$  sec and up to  $\tau = 0.55$  sec the value of the derivative  $dT/d\tau$  remains at an approximately constant level for each thermocouple, as also follows from Eq. (3). The beginning of the transition from the nonlinear mode to the linear mode of heating was determined from the plot of the derivative  $dT/d\tau$  since in the plot of  $T(\tau)$  this transition is not sufficiently distinct. In Fig. 3b, one can observe a difference ( $\sim 10\%$ ) in the measured values of the derivative  $dT/d\tau$ , which is slightly higher for the thermocouple located closer to the surface; this is due to the insulation failure caused by the electric arc, which leads to an increase in the measurement error. Burning-out of the insulation is the main reason for the scatter of experimental points in this experiment.

Figure 4 shows a typical time variation of the temperature of the cathode and the auxiliary rings. As the plot shows, the heating rate of the cathode substantially exceeds that of the auxiliary rings. This means that the heat flux arriving through the spot is significantly larger than the radiative and convective heat fluxes incident on the rings beyond the arc spot. As was mentioned earlier, the share of the radiative-convective heat flux was less than 30%, which favored improvement of accuracy in the volt-equivalent determination.

Figure 5 presents results of experiments carried out on the GWIPh setup (points 1); the same figure compares them with data obtained on the experimental setup of the A. V. Luikov Heat and Mass Transfer Institute (hereafter HMTI) of the National Academy of Sciences of Belarus and published in [2] (points 2). The experimental points of [2] are obtained within the range of magnetic fields of 0.133–0.95 T using a slightly modified procedure, namely, the method of variation of the cathode-ring width (see [2]). Moreover, they are current-averaged according to the results of up to 80 measurements with a current variation from 25 to

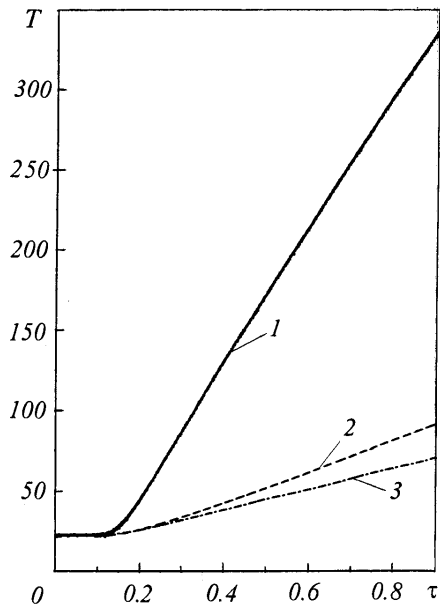


Fig. 4. Time plots of the recorded temperatures  $T$  of cathode ring 1 and auxiliary calorimetric rings 2 and 3.

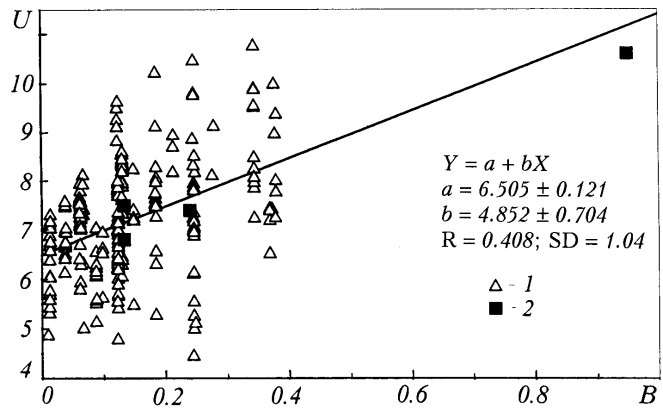


Fig. 5. Thermal volt-equivalent of the arc spot on the copper cathode  $U$  as a function of the magnetic field: 1) results of experiments on the GWIPh setup; 2) results of experiments on the HMTI setup.  $U$ , V;  $B$ , T.

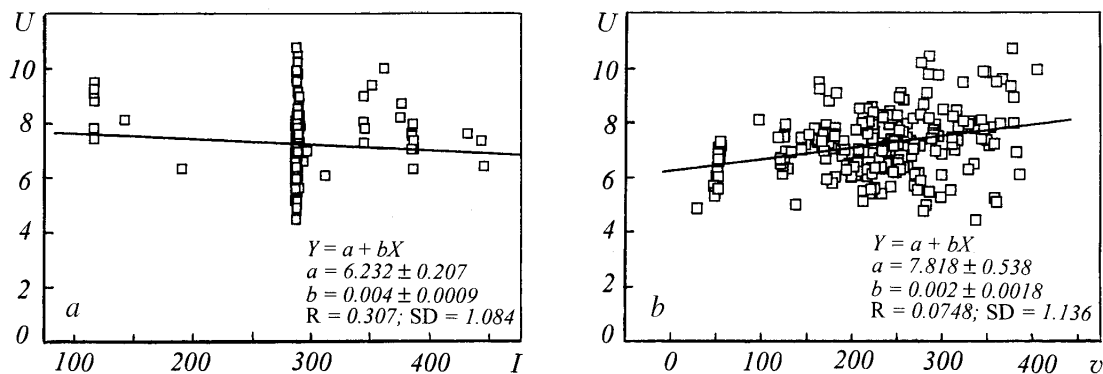


Fig. 6. Thermal volt-equivalent of the arc spot on the copper cathode  $U$  as a function of: a) current  $I$  and b) velocity  $v$  of the displacement of the arc spot as determined from results of experiments on the GWIPh setup.  $I$ , A;  $v$ , m/sec.

1000–1500 A for each point. The averaging in [2] was carried out by applying a linear approximation of the heat flux toward the cathode as a function of the current in the form  $Q_1 = cI$ . This presumed constancy of the volt-equivalent  $U$ , which is the main component (about 70%) of the angular coefficient  $c$ . The experimental points obtained on the GWIPh setup have not been current-averaged and therefore have a substantially larger scatter (see Fig. 5). Despite this, the results of a linear approximation of the magnetic field of 239 experiments on the GWIPh setup in the form

$$U = a + bB$$

are quite consistent with the result presented in [2] (see Fig. 5). Thus, in [2] the authors obtained  $a = 6.52$  and  $b = 4.28$ , while, according to Fig. 5,  $a = 6.5 \pm 0.1$  and  $b = 4.9 \pm 0.7$  (an error of up to 14%), although the GWIPh results have a high variance. For the 239 points the standard deviation is 1.0395 with a correlation coefficient of 0.409.

As was been mentioned above, in [2] the authors used the assumption of the independence of the thermal volt-equivalent  $U$  from the current strength. For comparison purposes, Fig. 6a shows results of linear approximation of the volt-equivalent  $U$  as a function of the current strength according to the data of our experiments carried out on the GWIPh setup. The angular coefficient and the correlation coefficient for this approximation approach zero. This agrees with the assumption adopted in [2].

The velocity of an arc moving in a magnetic field along a closed trajectory around the electrodes depends not only on the magnetic field but also on the axial velocity of the gas in the electrodes [10]. On the GWIPh setup, the arc velocity was varied from 28 to 400 m/sec by varying both the magnetic field and the axial air velocity. Therefore it is of interest to know what had a more substantial effect on the equivalent – the velocity of the displacement of the arc relative to the electrode or the magnitude of the external magnetic field in which the arc moved. Figure 6b shows results of linear approximation of the volt-equivalent  $U$  as a function of the arc velocity according to the data of the same experiments on the GWIPh setup. The correlation coefficient is seen to deteriorate as compared to the correlation for the magnetic field (0.3 instead of 0.4). Apparently, the magnetic field has a more substantial effect on the thermal volt-equivalent than the linear velocity of arc displacement relative to the cathode.

**Conclusion.** It has been confirmed experimentally that the magnetic field applied for the displacement of the arc in electric-arc heaters of a gas has an effect on the heat flux in the arc spot on the copper cathode and that this effect can be approximated by a simple linear dependence of the cathode thermal volt-equivalent on the magnetic induction. The new results confirm data obtained previously using other experimental methods and can be used in calculations of optimum operating regimes for a copper cathode with minimum erosion, for instance, according to the procedures described in [7].

We express our thanks to A. A. do Prado and J. B. Pineiro for their technical assistance in this work. We acknowledge the financial support of the Scientific Funds CNPq, FAPESP, and FINEP of Brazil.

## NOTATION

$U$ , thermal volt-equivalent, V;  $\Delta U_c$ , near-cathode voltage drop, V;  $B$ , magnetic induction, T;  $I$ , strength of the current, A;  $W$ , dimensionless enthalpy of ablation of the electrode material;  $f$ , dimensionless criterion characterizing the degree of fusion of the electrode surface and the transition of the cathode spot from the first type to the second type;  $g_0$ , specific cathode erosion in a spot of the first kind,  $\text{kg}\cdot\text{C}^{-1}$ ;  $g$ , specific cathode erosion in a spot of the second kind,  $\text{kg}\cdot\text{C}^{-1}$ ;  $h_{ef}$ , effective enthalpy of ablation of the electrode material,  $\text{J}\cdot\text{kg}^{-1}$ ;  $T_f$ , fusion temperature of the cathode material, K;  $T$ , electrode temperature, K;  $\gamma$ , current density,  $\text{A}\cdot\text{m}^{-2}$ ;  $\lambda$  and  $a$ , thermal conductivity and thermal diffusivity of the cathode material, respectively,  $\text{W}\cdot\text{m}^{-1}\cdot\text{K}^{-1}$ ,  $\text{m}^2\cdot\text{sec}^{-1}$ ;  $v$ , velocity of the arc spot,  $\text{m}\cdot\text{sec}^{-1}$ ;  $Q$ , total heat flux toward the calorimeter, W;  $Q_s$ , heat flux toward the cathode arc spot, W;  $Q_1$ , total measured heat flux toward calorimetric ring 1, W;  $q_1$ ,  $q_2$ , and  $q_3$ , densities of the heat flux toward the corresponding calorimetric rings,  $\text{W}\cdot\text{m}^{-2}$ ;  $x$ , axial coordinate reckoned from the cathode middle cross section downstream, m;  $F$ , area of the heat-absorbing interior surface of the calorimetric ring,  $\text{m}^2$ ;  $Q_{1rc}$  and  $q_{1rc}$ , radiative-convective heat flux and its density in calorimetric ring 1 (cathode) (see Figs. 1 and 2), W,  $\text{W}\cdot\text{m}^{-2}$ ;  $R_1$ ,  $R_2$ , and  $r$ , inner, outer, and running radii of the calorimetric ring, respectively, m;  $\tau$ , time, sec;  $J_i$ ,  $Y_i$ , first- and second-kind Bessel functions of the  $i$ -th order;  $R$ , correlation coefficient; SD, standard deviation. Subscripts: ef, effective value; f, fusion; 0, initial value; s, spot; 1, 2, 3, ordinal number of the ring calorimeter with respect to the distance from the cathode; rc, radiative-convective.

## REFERENCES

1. J. D. Cobine, *Gaseous Conductors*, New York (1958).
2. L. I. Sharakhovskii (Sharakhovsky), A. Marotta, and V. N. Borisyuk, *J. Phys. D: Appl. Phys.*, **30**, 2018-2025 (1997).
3. A. Marotta and L. I. Sharakhovskii (Sharakhovsky), *J. Phys. D: Appl. Phys.*, **29**, 2395-2403 (1996).



4. A. Marotta, L. I. Sharakhovskii (Sharakhovsky), and A. M. Esipchuk (Essiptchouk), *Annals New York Acad. Sci.* **891**, 36-42 (1999).
5. V. I. Rakhovskii, *IEEE Trans. Plasma Science*, **PS-4**, No. 2, 81-102 (1976).
6. V. I. Rakhovskii, *Izv. Sib. Otd. Akad. Nauk SSSR, Ser. Tekh. Nauk*, **1**, No. 3, 11-27 (1975).
7. L. I. Sharakhovskii (Sharakhovsky), A. Marotta, and V. N. Borisyyuk, *J. Phys. D: Appl. Phys.*, **30**, 2421-2430 (1997).
8. A. V. Luikov, *Theory of Heat Conduction* [in Russian], Moscow (1967).
9. E. P. Trofimov, *Inzh.-Fiz. Zh.*, **3**, No. 10, 47-53 (1960).
10. L. I. Sharakhovskii, *Inzh.-Fiz. Zh.*, **20**, No. 2, 306-313 (1971).